

Myosin Motors and Not Actin Comets Are Mediators of the Actin-based Golgi-to-Endoplasmic Reticulum Protein Transport^D

Juan M. Durán,^{*} Ferran Valderrama,^{*†} Susana Castel,[‡] Juana Magdalena,[§] Mónica Tomás,^{||} Hiroshi Hosoya,[¶] Jaime Renau-Piqueras,^{||} Vivek Malhotra,[#] and Gustavo Egea^{*@}

^{*}Departament de Biologia Cel·lular i Anatomia Patològica, Facultat de Medicina, Institut d'Investigacions Biomèdiques August Pi i Sunyer, Universitat de Barcelona, E-08036 Barcelona, Spain; [‡]Serveis Científic-Tècnics, Universitat de Barcelona, E-08028 Barcelona, Spain; [§]School of Biosciences, Molecular Cell Division, University of Birmingham, Birmingham B15–2TT, United Kingdom; ^{||}Centro de Investigación, Hospital La Fe, E-46009 Valencia, Spain; [¶]Department of Biological Science, Graduate School of Science, Hiroshima University, 739-8526 Hiroshima, Japan; and [#]Department of Biology, University of California San Diego, La Jolla, California 92093

Submitted April 18, 2002; Revised October 4, 2002; Accepted October 21, 2002
Monitoring Editor: Anthony P. Bretscher

We have previously reported that actin filaments are involved in protein transport from the Golgi complex to the endoplasmic reticulum. Herein, we examined whether myosin motors or actin comets mediate this transport. To address this issue we have used, on one hand, a combination of specific inhibitors such as 2,3-butanedione monoxime (BDM) and 1-[5-isoquinoline sulfonyl]-2-methyl piperazine (ML7), which inhibit myosin and the phosphorylation of myosin II by the myosin light chain kinase, respectively; and a mutant of the nonmuscle myosin II regulatory light chain, which cannot be phosphorylated (MRLC2^{AA}). On the other hand, actin comet tails were induced by the overexpression of phosphatidylinositol phosphate 5-kinase. Cells treated with BDM/ML7 or those that express the MRLC2^{AA} mutant revealed a significant reduction in the brefeldin A (BFA)-induced fusion of Golgi enzymes with the endoplasmic reticulum (ER). This delay was not caused by an alteration in the formation of the BFA-induced tubules from the Golgi complex. In addition, the Shiga toxin fragment B transport from the Golgi complex to the ER was also altered. This impairment in the retrograde protein transport was not due to depletion of intracellular calcium stores or to the activation of Rho kinase. Neither the reassembly of the Golgi complex after BFA removal nor VSV-G transport from ER to the Golgi was altered in cells treated with BDM/ML7 or expressing MRLC2^{AA}. Finally, transport carriers containing Shiga toxin did not move into the cytosol at the tips of comet tails of polymerizing actin. Collectively, the results indicate that 1) myosin motors move to transport carriers from the Golgi complex to the ER along actin filaments; 2) nonmuscle myosin II mediates in this process; and 3) actin comets are not involved in retrograde transport.

Article published online ahead of print. Mol. Biol. Cell 10.1091/mbc.E02-04-0214. Article and publication date are at www.molbiolcell.org/cgi/doi/10.1091/mbc.E02-04-0214.

^D Online version of this article contains supplementary data. Online version available at www.molbiolcell.org.

[†] Imperial Cancer Research Fund, 44 Lincoln's Inn Fields, London WC2A 3PX, England.

[@] Corresponding author. E-mail address: egea@medicina.ub.es.

INTRODUCTION

Actin filaments are crucial for cell migration and the maintenance of cellular morphology. In addition, a role for actin in membrane trafficking is emerging for both the endocytic and the secretory pathway (for recent reviews, see DePina and Langford, 1999; De Matteis and Morrow, 2000; Qualmann *et al.*, 2000; Apodaca, 2001; May and

Machesky, 2001; Stamnes, 2002). Although the role of actin in the secretory pathway has long been elusive, a breakthrough in our understanding has come with the use of highly specific inhibitors of actin polymerization, such as latrunculins and botulinum C2 toxin. Thus, actin filaments play a significant role in basolateral and Golgi-to-endoplasmic reticulum (ER) protein transport in polarized and nonpolarized mammalian cells, respectively (Müsch *et al.*, 1997, 2001; Valderrama *et al.*, 2000, 2001). Additional results that substantiated the involvement of actin in membrane trafficking in mammalian cells stem from the presence of members of myosin superfamily in organelle and vesicle transport in the secretory and endocytic pathways. For example, myosin V transports ER-derived vesicles in nerve cells (Tabb *et al.*, 1998) and interacts with synaptic vesicle proteins (Prekeris and Terrian, 1997; Miller and Sheetz, 2000); myosin I was initially detected in isolated Golgi fractions and vesicles (Fath and Burgess, 1993; Fath *et al.*, 1994; Montes de Oca *et al.*, 1997), although it seems to be functionally and structurally involved in the endocytic pathway (Cordonnier *et al.*, 2001, and references therein); myosin VI has been localized in the Golgi complex (Buss *et al.*, 1998) but to date has only been shown to be functionally involved in clathrin-mediated endocytosis (Buss *et al.*, 2001); and finally, myosin II has been implicated in the formation of and immunolocalized in *trans*-Golgi-derived transport carriers (Narula and Stow, 1995; Ikonen *et al.*, 1996, 1997; Ecay *et al.*, 1997; Müsch *et al.*, 1997; Heimann *et al.*, 1999), although with controversial results (Simon *et al.*, 1998; Stow *et al.*, 1998). Taken together, these results suggest that myosins are involved in intracellular trafficking by binding to subcellular compartments and generating force, either in the formation or the movement of vesicular carriers.

Until recently, the only known mechanism by which membrane structures moved along actin tracks was the myosin motors. However, the molecular mechanisms for the intracellular movement of certain pathogens through the formation of actin comets (for recent reviews, see Cossart, 2000; Goldberg, 2001) have also been observed in secretory and endocytic vesicles (Merrifield *et al.*, 1999, 2001; Rozelle *et al.*, 2000; Taunton *et al.*, 2000; Orth *et al.*, 2002; Benesch *et al.*, 2002; Lee and De Camilli, 2002). An actin comet is a characteristic structure easily visible by light microscopy, which results from a focalized actin polymerization (the tail) onto endomembranes and that acts as a driving force to propel them through the cytoplasm (for review, see Taunton, 2001). Vesicle rocketing basically requires N-WASP and Arp2/3 (Rozelle *et al.*, 2000; Benesch *et al.*, 2002). We have recently reported that N-WASP/Arp2/3 regulates Golgi-to-ER protein transport (Luna *et al.*, 2002), and, therefore, it is possible that actin comets propel Golgi-to-ER transport carriers (for review, see Ridley, 2001).

Herein, we examine whether myosin motors, which exert force against actin filaments, move these Golgi-to-ER transport carriers or, in contrast, they are propelled by actin comets, as occurs with some pathogens. The results indicate that only myosin motors move to transport carriers along actin filaments in the Golgi-to-ER pathway. In addition, we provide direct evidence that nonmuscle myosin II is involved in this process.

MATERIALS AND METHODS

Materials

Cy3-tagged native Shiga toxin fragment B was obtained from Ludger Johannes and Bruno Goud (Institute Curie, Paris, France; Johannes *et al.*, 1997). The plasmid encoding myc-tagged mouse PIP5-KI α (PIP5K) was from Laura M. Machesky (University of Birmingham, Birmingham, United Kingdom; Rozelle *et al.*, 2000), and the plasmids encoding myc-tagged MRLC2 wild-type (MRLC2^{wt}) and nonphosphorylated (MRLC2^{AA}) forms were generated by site-directed mutagenesis by using polymerase chain reaction as described previously (Iwasaki *et al.*, 2001). Antibodies against the myc-epitope were from 9E10 hybridoma, and those to Golgi-resident proteins giantin, mannosidase II, and galactosyltransferase were supplied by H.-P. Hauri (Biozentrum, Basel, Switzerland), K. Moremen (University of Georgia, Athens, GA), and E. Berger (University of Zürich, Zürich, Switzerland), respectively. DMEM and fetal calf serum (FCS) were from Invitrogen (Paisley, UK); secondary Alexa-488 or Alexa-546 F(ab')₂ fragments, cascade blue dextran, tetramethylrhodamine B isothiocyanate (TRITC)-dextran (10,000 mol. wt.), Fluo-4/acetoxymethyl ester (AM), and Pluronic F-127 were from Molecular Probes (Leiden, The Netherlands); 2,3-butanedione monoxime (BDM) was purchased from Sigma-Aldrich (St. Louis, MO); and Mowiol, thapsigargin, 1-[5-isoquinoline sulfonyl]-2-methyl piperazine (ML7), H7, and H89 were from Calbiochem (Nottingham, United Kingdom). Of note, BDM was reconstituted in DMEM (concentrated stock of 250 mM), H7 (10 mM) in distilled water, and ML7 and H89 (10 mM each) in a mixed solution of distilled water and ethanol (1:1). Unless otherwise stated, all other chemicals were from Sigma-Aldrich.

Cell Culture

HeLa and normal rat kidney (NRK) cells were cultured in DMEM containing 10% FCS supplemented with 10 mM L-glutamine, penicillin (100 U/ml), and streptomycin (100 μ g/ml). Cells were grown in a humidified incubator at 37°C and 5% CO₂.

Microinjection Experiments

For microinjection, HeLa and NRK cells were grown for 1–2 d on normal glass coverslips and cultured in DMEM plus 10% FCS containing 25 mM HEPES, and supplemented with penicillin, streptomycin, and glutamine. Myc-tagged PIP5K cDNA constructs were first diluted to 50 ng/ml and then microinjected into the cell nucleus with an automated microinjection system (Carl Zeiss, Jena, Germany). After microinjection, the coverslips were transferred to a Petri dish containing fresh culture medium and returned to the incubator.

Expression of Recombinant MRLC2

HeLa cells were transfected using Superfect reagent (QIAGEN, Valencia, CA) following the protocol indicated by the manufacturer. Briefly, cells plated on p35 culture Petri dishes were incubated for 2 h with MRLC2^{wt} or MRLC2^{AA} cDNAs (2 μ g) previously mixed with Superfect in DMEM containing 10% of FCS. Subsequently, cells were washed and cultured in DMEM for 16–24 h.

Intracellular Calcium Measurements

NRK cells were plated onto glass-bottom dishes (Delta T culture dishes; Bioprotechs, Butler, PA). After 1 d of culture, cells were rinsed three times with loading buffer (Hanks balanced salt solution with 10 mM D-glucose, 1.3 mM CaCl₂, and 1.1 mM MgCl₂) and loaded with Fluo-4/AM (4 μ M) dissolved in loading buffer containing 0.4% Pluronic for 15 min at 37°C in a 5% CO₂ atmosphere. Cells were then washed in loading buffer and incubated in DMEM for 30 min at room temperature to allow complete deesterification of intracellular AM ester. All calcium measurement experiments were carried out at

Table 1. Stereological analysis of the Golgi complex in control and BDM- or ML7-treated NRK cells

	BDM			ML7	
	Control	20 mM	40 mM	15 μ M	30 μ M
Vv tGC/cyt	3.9 \pm 2.7	17 \pm 4.3	23 \pm 5.4	19.4 \pm 6.3	21.3 \pm 8
Vv cist/cyt	48.8 \pm 7.6	60.4 \pm 10	58.4 \pm 10	60.1 \pm 12.1	68 \pm 11.2
Sv cist/tGC	9.3 \pm 2.7	8 \pm 3.1*	5 \pm 1.2	4.8 \pm 1	4.9 \pm 1
Vv ves/tGC	3.0 \pm 0.8	6.2 \pm 2	5.8 \pm 2.2	7.8 \pm 3.3	14 \pm 3.3
N	40	47	43	44	44

Vv: volume density (%); Sv: surface density (μm^{-1}); Cist: Golgi cisternae; ves: per-Golgi vesicular structures. cyt: cytoplasm; N, number of cells analyzed. All values are statistically significant ($p \leq 0.05$) except where indicated respect to control cells (*).

37°C (Delta T; Biophtechs) adapted to an inverted TCS 4D confocal microscope (Leica Microsystems, Heidelberg, Germany). Images were taken with a Plan Apochromatic 40 \times /1.3 oil objective by using the Ion Domain Quantify software from Leica Microsystems. Regions of Interest (ROIs) were set for each cell. Background-subtracted, fluorescence signals of each ROI were corrected for the bleaching of the Fluo-4 fluorescence signal and the mean fluorescence intensity of each ROI was calculated. Changes in the intracellular calcium concentration ($[\text{Ca}^{2+}]_i$) are given as the relative change in the fluorescence ratio F/F_0 of Fluo-4/AM, where F is the fluorescence intensity at any time, and F_0 is the baseline fluorescence intensity, as described previously (Bootman *et al.*, 1997; Heemsker *et al.*, 2001). Values are expressed as the mean \pm S.E. of the normalized fluorescence (F/F_0). Data were obtained from 8 to 30 cells.

VSV-G and Shiga Toxin Transport Assays

Infection with the temperature-sensitive (ts) mutant ts045 VSV was performed as described previously (Valderrama *et al.*, 1998). Indirect immunofluorescence transport of VSV-G from ER-to-Golgi complex was performed following Bonatti *et al.* (1989).

For the Shiga toxin (ST-B-KDEL) transport experiments, HeLa cells were first incubated in binding medium (FCS-free DMEM) and treated with cy3-ST-B-KDEL-fragment for 30 min at 4°C, and the unbound toxin was then washed for 5 min in ice-cold phosphate-buffered saline. Thereafter, cells were incubated with DMEM at 20°C for 2 h to accumulate the internalized ST-B-KDEL in early/recycling endosomes. They were then transferred to 37°C to synchronize the ST-B-KDEL transport to the ER via the Golgi complex.

Indirect Immunofluorescence

Indirect immunofluorescence was carried out as described previously (Valderrama *et al.*, 1998, 2000) with the following antibody dilutions: anti- β -coatamer protein (COP), 1:60; anti-mannosidase II, 1:2000; anti-myc, 1:100; anti-galactosyltransferase, 1:500; anti-giantin, 1:500; anti-VSV-G, 1:50, and Alexa 488- and 546-conjugated secondary antibodies, 1:500 and 1:1000, respectively. TRITC- or coumarin-phalloidin were used to stain F-actin, at a dilution of 1:1000 and 1:100, respectively. The coverslips were mounted on microscope slides using Mowiol. Microscopy and imaging were performed with a BX60 epifluorescence microscope with a chilled DP-50 charge-coupled device camera (Olympus, Tokyo, Japan) or a TCS-NT confocal microscope (Leica Microsystems). The images were processed on PC computers using Adobe Photoshop 5.0.

Electron Microscopy and Stereological Analyses

Cells were washed twice in 100 mM cacodylate buffer (pH 7.2) and fixed with 2.5% glutaraldehyde in this buffer for 60 min at room temperature. Cells were then washed (3 \times 5 min each) in cacodylate

buffer and postfixed with 1% (vol/vol) OsO_4 /1.5% (wt/vol) $\text{K}_4\text{Fe}(\text{CN})_6$ in 100 mM cacodylate buffer for 1 h at 4°C. Cells were scraped, pelleted, and treated for 1 h at 4°C with 1% tannic acid in cacodylate buffer, rinsed in distilled water, and stained en bloc with 1% aqueous uranyl acetate for 1 h, followed by dehydration through graded ethanol solutions and embedding in Epon 812. Ultrathin sections were stained with lead citrate for 2 min and observed in a 301 electron microscope (Philips, Eindhoven, The Netherlands). Randomly selected micrographs were taken at the same final magnification (47,500 \times) and analyzed using point-counting procedures. The Golgi complex (GC) was defined as a group of cisternae organized in stacks with tubular and vesicular structures. Total Golgi complex (tGC) was defined as an area containing at least one cisterna and peri-Golgi vesicles, with an arbitrary border in the cytoplasm surrounding the Golgi (Renau-Piqueras *et al.*, 1987). Intermediate elements in continuity with the rough ER were excluded. The stereological parameters were determined using standard procedures (Renau-Piqueras *et al.*, 1987). The minimum sample size (number of micrographs; Table 1) of each stereological parameter was determined by the progressive mean technique (confidence limit of 5%). The results were expressed as means \pm SD and compared using the Student's *t* test.

RESULTS

Myosin Inhibition Alters the Golgi Complex Morphology

To determine whether actin-dependent motors govern membrane dynamics at the ER/Golgi interface, we first used BDM as a broad-spectrum inhibitor of both conventional and unconventional myosin Mg^{2+} -ATPase activity (Higuchi and Takemori, 1989; Herrmann *et al.*, 1992; Cramer and Mitchison, 1995; Lin *et al.*, 1996). At fluorescence level, NRK cells treated with BDM at concentrations ranging from 5 to 20 mM showed no change in the Golgi complex morphology in comparison with untreated control cells (Figure 1, A and C), but at higher concentrations (30 and 40 mM) the Golgi complex showed a more compact morphology (Figure 1E). Actin stress fibers were virtually unaltered when cells were treated with BDM from 5 to 20 mM (Figure 1D), but they diminished in number when it was used at 40 mM (Figure 1F).

Because myosin II, a major actin-based motor protein, has been implicated in the formation of transport vesicles at the *trans*-Golgi network (TGN) level (Müsch *et al.* 1997; Stow *et al.*, 1998), we then examined the effect of ML7, a compound that inhibits myosin light chain kinase (MLCK) function,

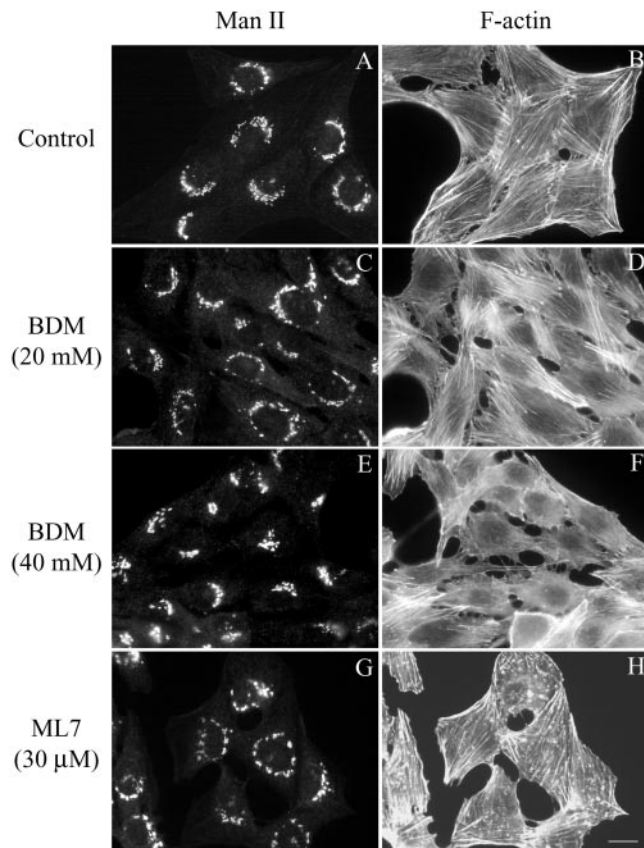


Figure 1. Double immunofluorescence microscopy experiments in untreated (A and B) and BDM- (C–F) or ML7-treated NRK cells (G and H) stained with anti-mannosidase II polyclonal antibodies (A, C, E, and G) and TRITC-phalloidin (B, D, F, and H) to reveal the Golgi-resident enzyme (Man II) and filamentous actin (F-actin), respectively. Bar, 10 μm .

thus specifically preventing myosin II activation via phosphorylation (Saitoh *et al.*, 1987). When NRK cells were treated with ML7 at concentrations of 15 and 30 μM , the Golgi complex was perinuclear but, instead of showing its continuous reticular shape characteristic of untreated NRK cells (Figure 1A), a pearl necklace-like morphology was observed (Figure 1G). Furthermore, ML7 also decreased actin stress fibers (Lamb *et al.*, 1988) and produced numerous actin-stained cytoplasmic spots (Figure 1H).

To determine the site and mode of action of BDM and ML7, an ultrastructural (Figure 2) and stereological analysis (Table 1) of the Golgi complex was performed. BDM at 20 or 40 mM induced severe changes in the Golgi ultrastructure, the cisternae seeming swollen (Figure 2B). BDM increased the volume occupied by the tGC in the cytoplasm (Vv tGC/cyt; Table 1). This could be attributable to an increase either in the volume of Golgi cisternae (Vv cist/tGC) or in the volume of peri-Golgi vesicular structures (Vv ves/tGC). At the electron microscopic (EM) level, the former is visualized as swollen cisternae (Figure 2B) and the latter results from the decrease in the Golgi membrane surface density (Sv cist/tGC). In cells treated with ML-7 (15 and 30 μM), similar

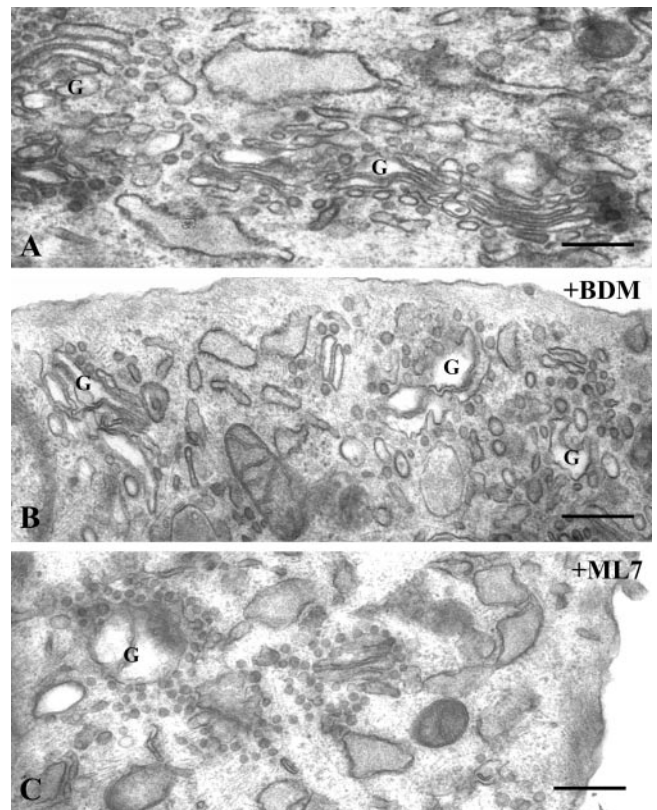


Figure 2. Electron microscopy of the Golgi complex in untreated (A) and BDM- (40 mM) or ML7 (30 μM)-treated NRK cells (B and C, respectively). Unlike control cells (A), BDM- (B) and ML7 (C)-treated cells show a Golgi complex with swollen cisternae (B) and numerous peri-Golgi vesicles. The latter are more evident after ML7 treatment (C), in which numerous peri-Golgi vesicles of uniform size and close attachment to the Golgi cisternae are easily observed.

results were obtained regardless of the concentration used, but the decrease in the Golgi membrane surface density (Sv cist/tGC) was greater. As expected, this was followed by a much higher volume density of peri-Golgi vesicular structures (Vv ves/tGC), which at the EM level are viewed as numerous vesicular structures of uniform size closely attached to Golgi cisternae (Figure 2C).

Inhibition of Myosin Function Alters the Retrograde, but Not the Anterograde, Protein Transport

Because actin filaments facilitate retrograde transport from the Golgi complex to the endoplasmic reticulum (Valderama *et al.*, 2001), we next studied whether myosin activation is required in ER/Golgi membrane dynamics. We first examined whether these antimyosin agents (BDM and ML7) alter the disassembly of the Golgi complex induced by brefeldin A (BFA) (Figure 3). NRK or HeLa cells were first treated with BDM and then with BFA for different times. BDM suppressed the disassembly of the Golgi complex induced by BFA (Figure 3, E–H and Q). To examine the involvement of myosin II in this membrane route, we ana-

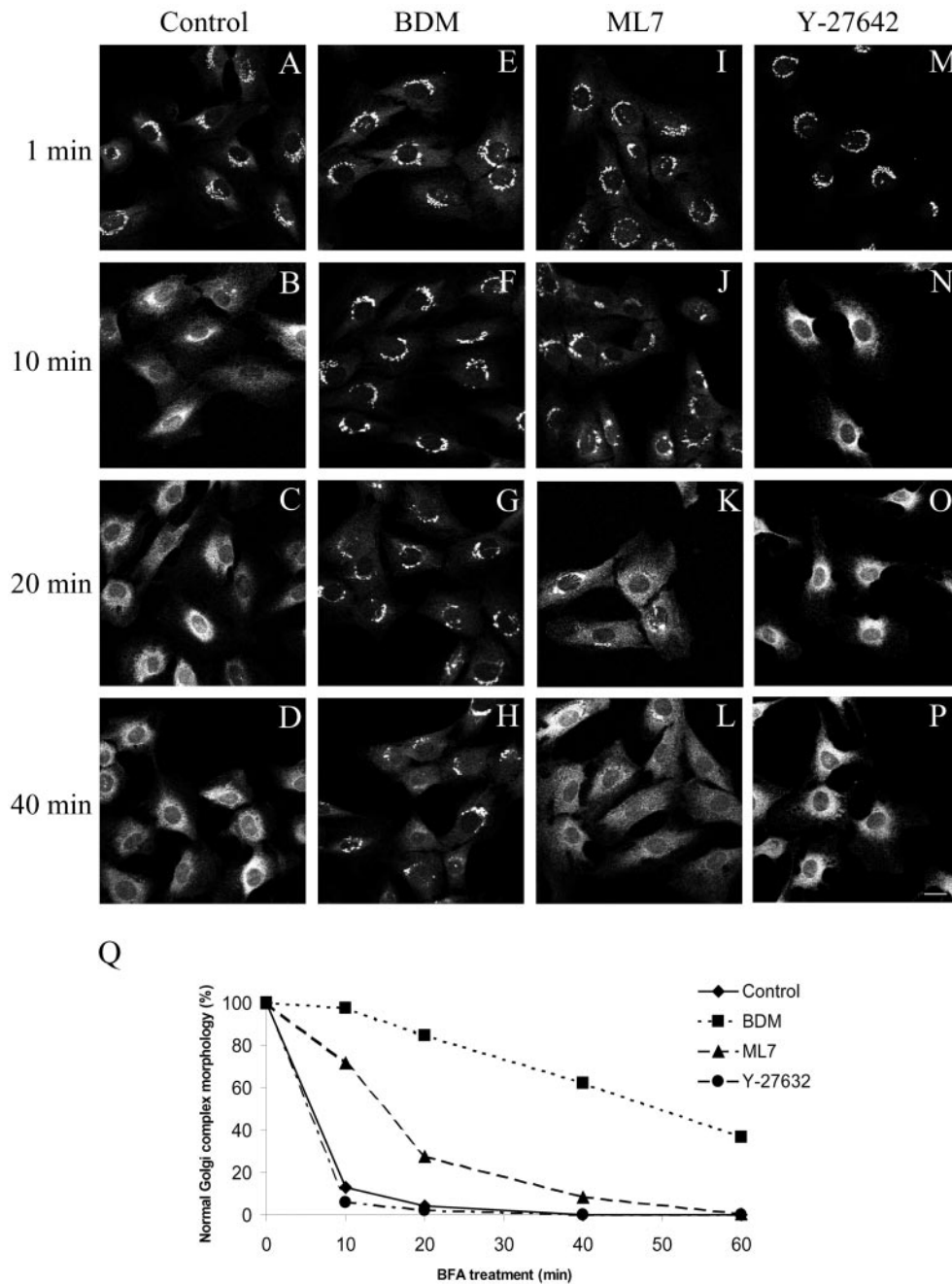


Figure 3. Immunofluorescence microscopy experiments of the kinetics of the BFA-induced disassembly of the Golgi complex stained to Man II in control (A–D), in BDM (20 mM)- (E–H), in ML7- (30 μ M) (I–L), and in Y-27642 (25 μ M)-treated NRK cell (M–P). A quantitative analysis of these results is shown in Q. The results are the mean of two independent experiments; at least 200 cells, randomly chosen, were counted per experimental condition. Note that the disassembly of the Golgi complex remained unaltered after treatment with the Rho kinase inhibitor Y-27642, but was significantly delayed by ML7 treatment and practically blocked by BDM. Bar, 10 μ m.

lyzed the effects of inhibiting MLCK by using ML7, and of overexpressing nonmuscle myosin II regulatory light chain (MRLC2) constructs. ML7 also produced a significant delay in the BFA-induced Golgi complex disassembly (Figure 3, I–L and Q), but its inhibitory effect was weaker than that

produced by BDM (Figure 3 Q). In addition to its effect on MLCK, ML7 is also able to partially inhibit protein kinase (PK) A and PKC enzymatic activities, albeit with a much lower efficiency than for MLCK (K_i values of 21 μ M, 42 μ M, and 300 nM, respectively). To examine whether PKA or PKC

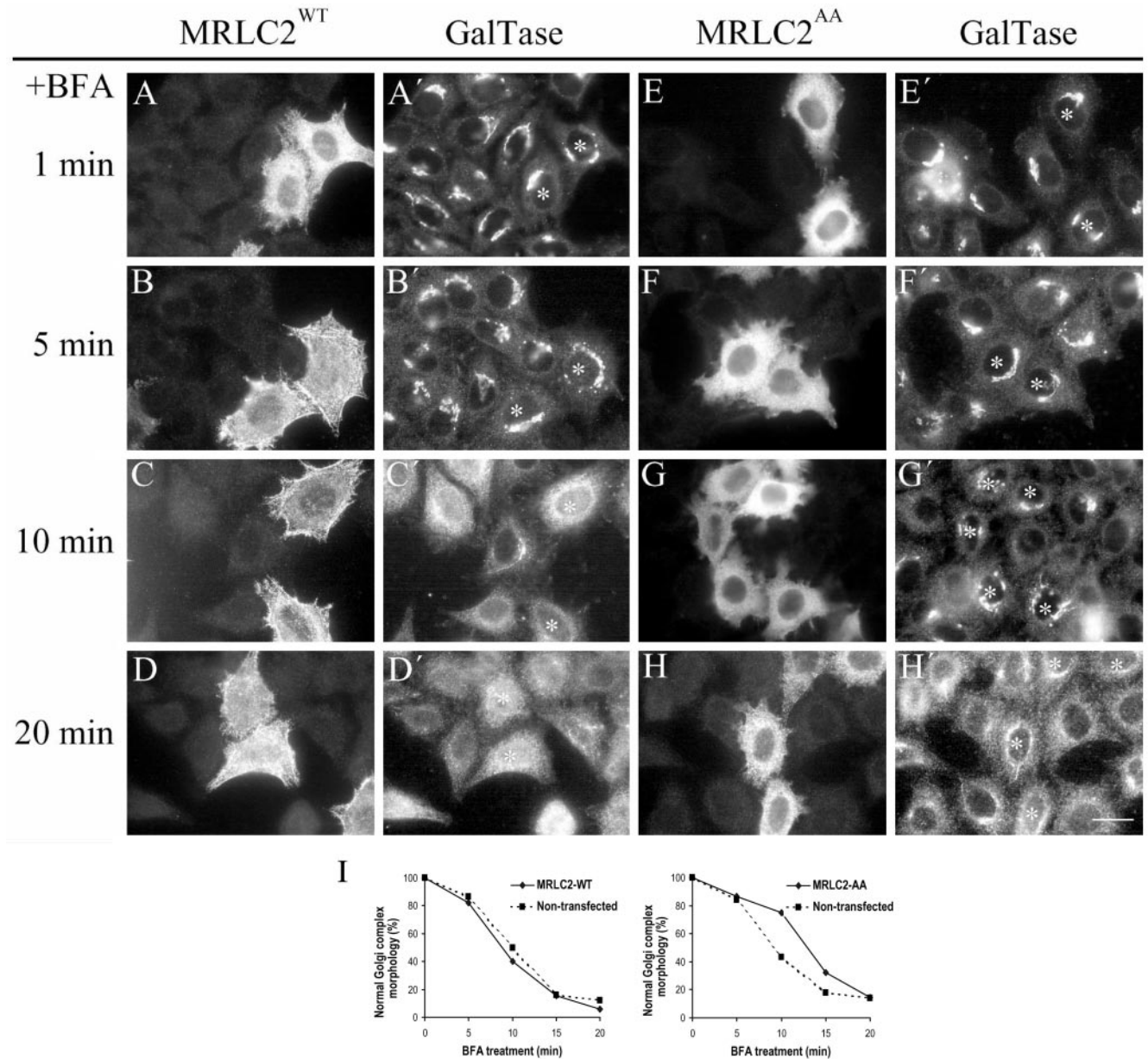


Figure 4. Kinetics of the BFA-induced disassembly of the Golgi complex stained to galactosyltransferase (galtase) in HeLa cells expressing myc-MRLC2^{wt} (A–D) or myc-MRLC2^{AA} (E–H). MRLC2 expressing cells were identified by immunofluorescence staining with anti-myc monoclonal antibodies (A–H) and the Golgi complex with anti-galtase polyclonal antibodies (A'–H'; asterisk indicates the corresponding transfected cell). A quantitative analysis of these results is shown in I (the results are the mean of two independent experiments). Note that the kinetics of the disassembly of the Golgi complex induced by BFA remains unaltered in cells expressing MRLC2^{wt}, but was delayed in MRLC2^{AA} in comparison with neighboring nontransfected cells. Bar, 10 μ m.

were also significantly involved in the retrograde pathway, NRK cells were treated with H7 or H89 (30 μ M). Neither H7- nor H89-treated cells altered the kinetics of the disassembly of the Golgi complex induced by BFA (see supplementary data). This suggests that neither PKA nor PKC is apparently involved in the Golgi-to-ER pathway.

To gain further insight into the involvement of nonmuscle myosin II, HeLa cells were transfected with either the re-

combinant myc-tagged MRLC2 wild-type (MRLC2^{wt}) or with a MRLC2 mutant that mimics its unphosphorylated state, in which both Ser19 and Thr18 were substituted by Ala (MRLC2^{AA}; Iwasaki *et al.*, 2001). The kinetics of the BFA-induced Golgi disassembly was greatly slowed down in cells expressing MRLC2^{AA} (Figure 4 F, F' to H, H'), whereas it remained unaltered in cells overexpressing the MRLC2^{wt} form (Figure 4 B, B' to D, D'). As expected, MRLC2^{AA}

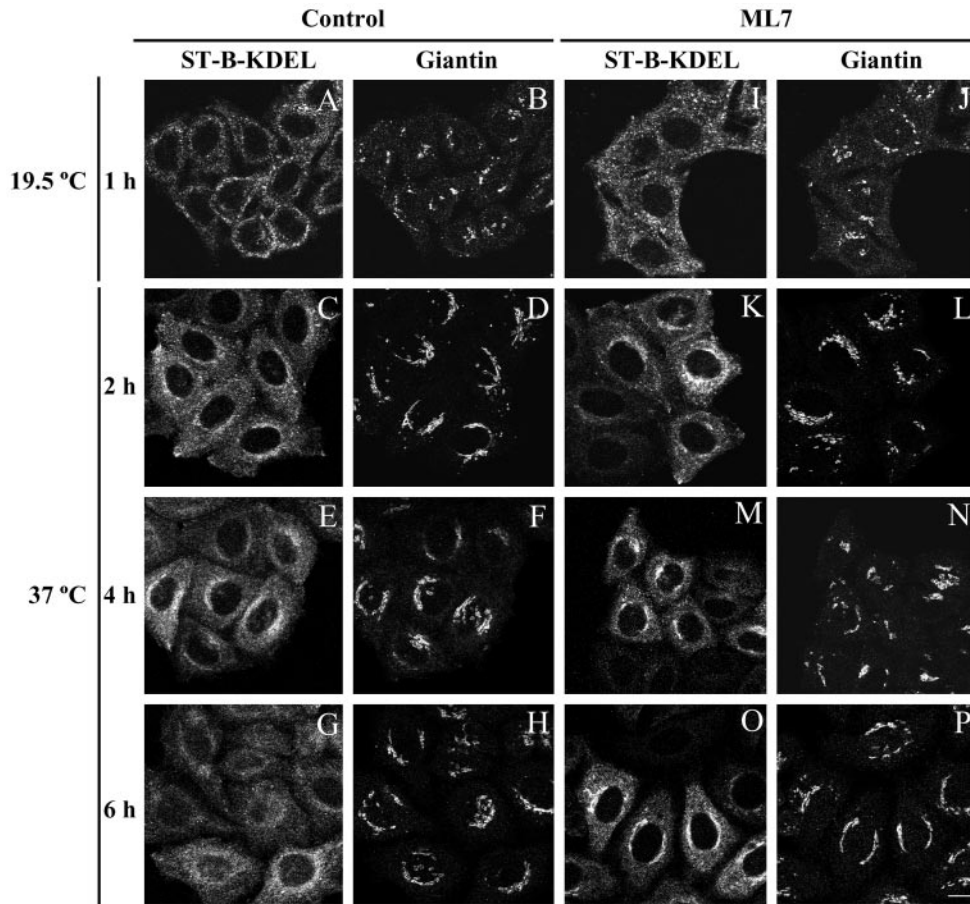


Figure 5. Double confocal immunofluorescence microscopy experiments of the retrograde transport kinetics of the cy3-tagged Shiga toxin fragment B containing the ER-retention signal KDEL (ST-B-Glyc-KDEL/ST-B-KDEL) in control (A–H) and ML7-treated HeLa cells (I–P). Plasma membrane internalization of the ST-B-KDEL was performed at 19.5°C to accumulate it in early/recycling endosomes (A, B, I, and J). Thereafter, cells were treated with ML7 (30 μ M) and treated and untreated cells were incubated at 37°C to trigger the transport of ST-B-KDEL to the ER through the Golgi complex, which was stained with anti-giantin monoclonal antibodies (B, D, F, H, J, L, N, and P). Notice that after 6 h, unlike in control cells (G and H), in ML7-treated cells (O and P) ST-B is still significantly located in the Golgi complex (O and P). Bar, 10 μ m.

reduced the presence of actin stress fibers stained with coumarin-phalloidin (our unpublished data), and it was mostly diffuse in the cytoplasm (Figure 4, E–H), whereas MRLC2^{wt} was mostly on actin stress fibers (Figure 4, A–D). Collectively, the results strongly indicate that nonmuscle myosin II is involved in the Golgi-to-ER pathway.

Next, we used Shiga toxin (ST-B) as a protein marker of the Golgi-to-ER pathway. Unlike NRK, HeLa cells bind Shiga toxin, which is transported to the ER via early endosomes and the Golgi complex (for review, see Sandvig and van Deurs, 2000). Cells were treated as reported previously and the toxin transport was imaged by confocal microscopy (Valderrama *et al.*, 2001). Briefly, cells were incubated at 4°C with cy3-tagged fragment B of the toxin bearing the KDEL sequence (ST-B-KDEL; Johannes *et al.*, 1997) and, after 30 min, incubated at 19.5°C for 1 h to accumulate the internalized toxin in the early/recycling endosomes. Subsequently, cells were treated with or without BDM (40 mM; our unpublished data) or ML7 (30 μ M; Figure 6) and thereafter

they were transferred to 37°C to synchronize the retrograde transport of Shiga toxin to the ER. In control cells (Figure 5, A–H), ST-B-KDEL travels from early/recycling endosomes (Figure 6A) via the Golgi complex (Figure 5, C–E) to the ER (Figure 5G) giving rise to the characteristic ER-like staining pattern as the toxin is retained. In contrast, in BDM- (our unpublished data) and in ML7-treated cells (Figure 5, I–O), after 6 h of transport, ST-B-KDEL was still clearly located in the Golgi complex (Figure 5O).

We next studied putative changes in the ER-to-Golgi membrane movement after myosin inhibition. To this end, NRK or HeLa cells were first treated with BFA to induce the fusion of Golgi membrane with ER, then incubated with BDM/ML7, and subsequently BFA was withdrawn from the culture medium. The rebuilding of the Golgi complex was visualized by fluorescence microscopy by using anti-mannosidase II (Man II) antibodies. No differences were observed in the kinetics of the reassembly of the Golgi complex either in cells treated with BDM or ML7 or in those express-

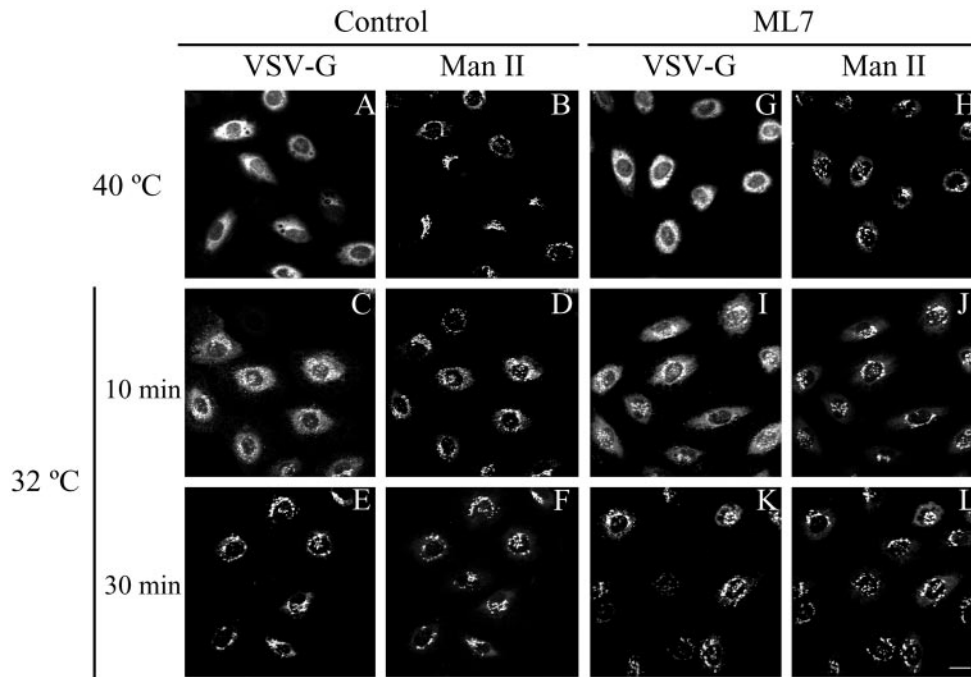


Figure 6. NRK cells were infected with the VSV ts045 temperature-sensitive mutant virus and after accumulation at 40°C VSV-G glycoprotein was monitored at immunofluorescence level with anti-VSV-G antibodies. Note that the kinetics of transport of VSV-G from the ER to the Golgi complex (stained to Man II) is the same in untreated (A, C, and E) and ML7-treated cells (G, I, and K). Bar, 10 μ m.

ing the MRLC2^{AA} mutant (our unpublished data). In addition, we assayed the ER-to-Golgi transport of the VSV-G protein by fluorescence microscopy with anti-VSV-G protein (Figure 6). Briefly, after infection of cells with ts045 mutant VSV, the cells were kept at nonpermissive temperature (40°C), at which the VSV-G protein is synthesized but retained in the ER, and then treated with BDM or ML7. Cells were shifted to the permissive temperature (32°C) and the intracellular location of VSV-G protein was monitored by fluorescence microscopy with an anti-VSV-G monoclonal antibody. Neither BDM (Figure 6) nor ML7 (our unpublished data) altered the transport of VSV-G protein from ER to the Golgi complex.

Taken together, the data strongly indicate that only myosins, and in particular nonmuscle myosin II, are involved in the Golgi-to-ER membrane pathway.

Neither BDM nor ML7 Alters the BFA-induced Coatomer Detachment or Tubule Formation

Treatment of cells with BFA leads to the formation of tubular extensions that have been implicated in the backflow of Golgi components to the ER. These tubules connect the two compartments and mediate the movement of Golgi lipids and proteins to the ER membranes where their membranes finally merge (Sciaky *et al.*, 1997). Because myosin II has been reported to be involved in the formation of vesicular carriers from the TGN (Müsch *et al.*, 1997; Stow *et al.*, 1998), we analyzed whether the formation of tubules from the Golgi complex induced by BFA was impaired by BDM or ML7. However, the first morphological event that is visualized in

cells treated with BFA is the release of COP components, such as β -COP from Golgi membranes, which is required for the redistribution of Golgi membranes into the ER (Donaldson *et al.*, 1990; Scheel *et al.*, 1997). Thus, it is conceivable that BDM and ML7 inhibit the BFA-mediated retrograde flow from the Golgi complex to the ER by inhibiting the release of coatomer from the Golgi complex. Therefore, we first carried out an immunofluorescence study using an anti- β -COP antibody on cells pretreated with BDM/ML7 or expressing MRLC2^{WT}/MRLC2^{AA}. BFA-induced release of β -COP from the Golgi complex was unaffected by BDM or ML7 (Figure 7, G and K, respectively) or MRLC2^{WT/AA} (our unpublished data). Regardless of whether cells were preincubated with BDM before BFA treatment or both agents were added simultaneously (see below), β -COP release was indistinguishable from that in cells treated with BFA alone (Figure 7C). β -COP was released at BFA incubation times, in which the Golgi complex remained morphologically unaffected (Figure 7, H and L), and neither BDM nor ML7 (Figure 7, E and I) nor MRLC2^{WT/AA} (our unpublished data) affected the distribution of the coatomer component.

We next analyzed the kinetics of the appearance of tubules from the Golgi complex when BDM- or ML7-treated cells were incubated with low concentrations of BFA (Figure 8). After 4 min of BFA treatment, the tubules were seen in both control and pretreated cells with BDM and ML7 (Figure 8, B, F, and J). After 6 min, the tubules were still visible in BDM/ML7-pretreated cells (Figure 8, G and K), although the characteristic ER-like staining pattern was already observed in some control cells (our unpublished data). After 10

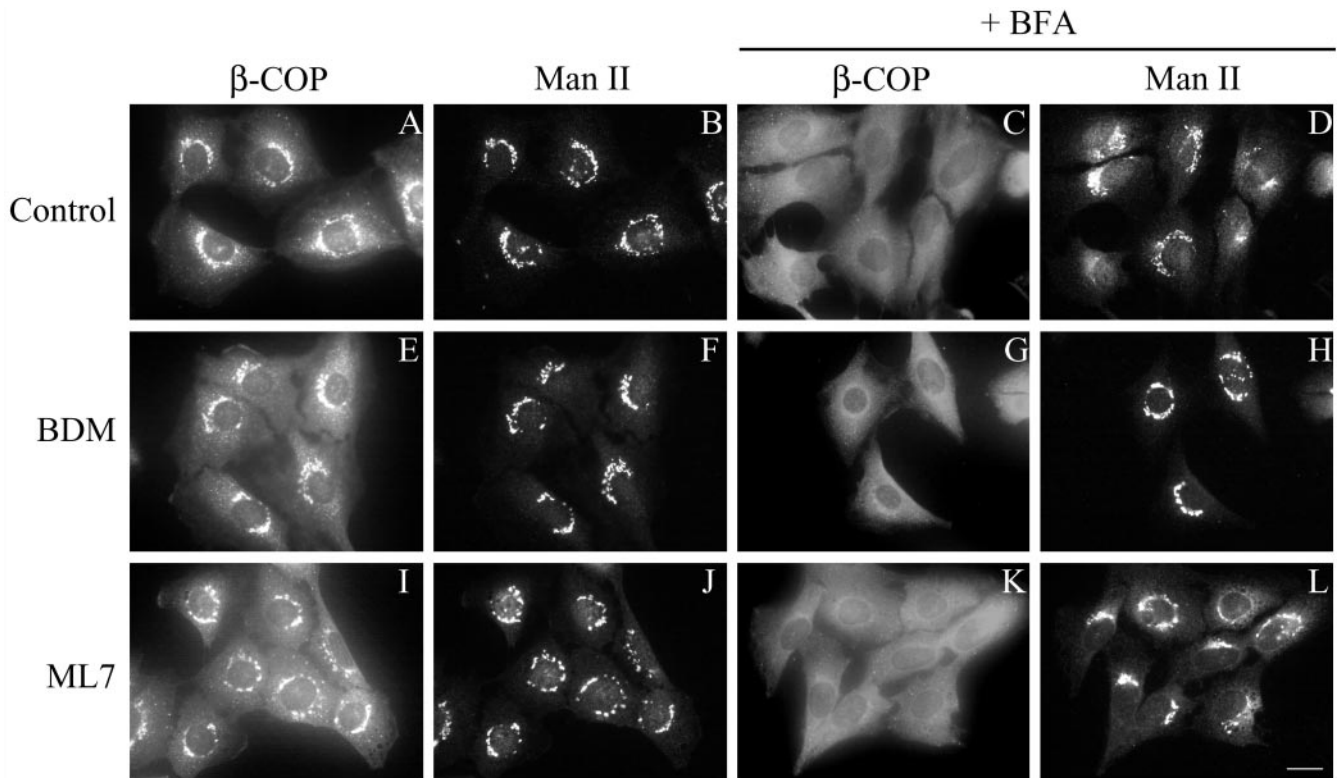


Figure 7. NRK cells were pretreated for 30 min with BDM (20 mM; E, F, G, and H) or ML7 (30 μ M; I, J, K, and L), and subsequently incubated with BFA (2 μ g/ml) for 60 s (C, D, G, H, K, and L). Thereafter, cells were fixed and processed for immunocytochemical double-staining by using antibodies against β -COP (A, E, I, C, G, and K) and to Man II (B, F, J, D, H, and L). Note that BDM and ML7 do not interfere with BFA-induced β -COP release (G and K) and they do not cause its release by themselves (E and I). Bar, 10 μ m.

min, most of the BDM- or ML7 plus BFA-treated cells still showed Man II-containing tubules and a Golgi structure was still clearly recognizable (Figure 8, H and L), whereas all the control BFA-treated cells showed the expected ER-like staining pattern for Man II (Figure 8D). The percentage of cells that showed Golgi-emerging tubules induced by BFA was unaltered by BDM or ML-7 treatments, but the tubules remained longer in the cytoplasm before their fusion with ER membranes (Figure 8M). Similarly, in MRLC2^{AA}-transfected and BFA-treated cells, long Golgi-derived tubules were still visualized when their neighboring nontransfected cells already displayed the characteristic ER-like staining pattern (Figure 4, G' and H').

BDM/ML7-induced Alteration in Golgi-to-ER Membrane Backflow Is Not Produced by Depletion of Intracellular Ca^{2+} Stores

Although BDM affects the actomyosin system and inhibits myosin ATPase in vitro (Higuchi and Takemori, 1989; Herrmann *et al.*, 1992; Cramer and Mitchison, 1995) and in vivo (Cramer and Mitchison, 1995; Lin *et al.*, 1996; Gloushankova *et al.*, 1998; Steinberg and McIntosh, 1998), it has also been reported that BDM affects intracellular calcium concentration (Steinberg and McIntosh, 1998, and references therein). This reported collateral effect of BDM on intracellular cal-

cium levels (in particular when it is used at higher concentrations of 30 mM; Phillips and Altschuld, 1996) could be relevant because the sequestration of Ca^{2+} to intracellular stores is required for the anterograde and retrograde transport between the ER and the Golgi complex (Beckers and Balch, 1989; Ivessa *et al.*, 1995; Chen *et al.*, 2002). Thus, to test whether the observed effects on the disassembly of Golgi induced by BDM or ML7 were the result of alterations in calcium homeostasis, we monitored in vivo the cytoplasmic calcium release from intracellular stores. HeLa cells were loaded with Fluo 4/AM and the fluorescence ratio was continuously monitored under the confocal microscope (Figure 9). Unlike ML7 (Figure 8C), BDM induced a small biphasic rise in $[Ca^{2+}]_i$ (1.34 ± 0.02 ; Figure 9, A and B). To assess the relative contribution of BDM to the $[Ca^{2+}]_i$ increase from the total Ca^{2+} from intracellular stores, cells were subsequently treated with thapsigargin, a selective inhibitor of the ER Ca^{2+} -ATPase, a pump that maintains a high concentration of Ca^{2+} in the lumen of the ER (Thastrup *et al.*, 1990). When thapsigargin was added 1.5 min after BDM, a much larger and monophasic rise in $[Ca^{2+}]_i$ was registered (4.1 ± 0.11 ; Figure 9A). When thapsigargin was added 30 min after BDM, a smaller peak was also observed but it lasted much longer (Figure 9B). After ML7 treatment, thapsigargin induced a small monophasic transient increase in $[Ca^{2+}]_i$ (2.1 ± 0.06 ; Figure 9C) regardless of the time

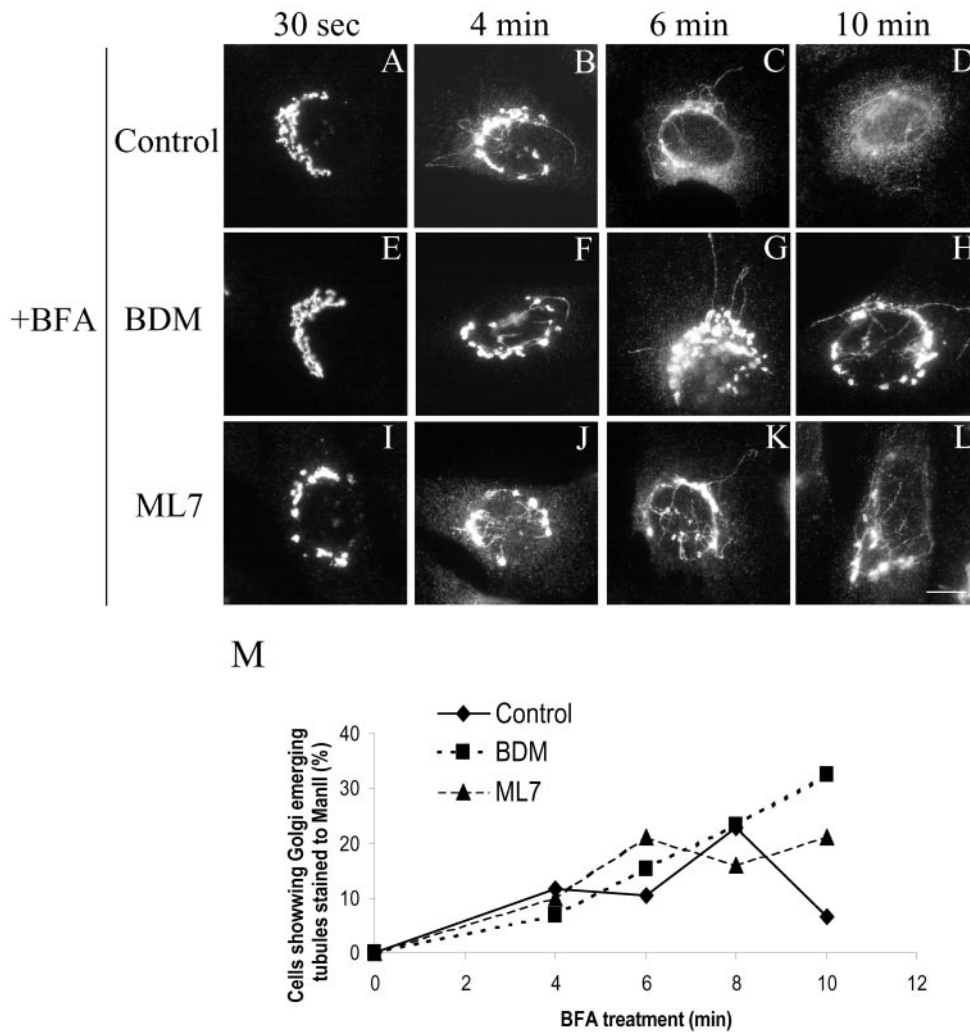


Figure 8. NRK cells were pretreated with BDM (20 mM) or ML7 (30 μ M) for 60 min and subsequently incubated with BFA (2 μ g/ml); at indicated times cells were fixed and stained for Man II. After 10 min, unlike BFA-treated cells alone (D), BDM/ML7-treated cells still showed Golgi-emerging tubules after BFA treatment (H and L, respectively). Notice that at earlier times (4 and 6 min) of BFA treatment both untreated and BDM/ML7-treated cells showed the normal appearance of BFA-induced tubules. A quantitative validation of these morphological observations is shown in M. This quantification is the mean of two independent experiments, 200 cells being counted in each one. Bar, 10 μ m.

interval used between the two compounds. Taking these results into account, we examined whether the effect of BDM on the disassembly of the Golgi complex induced by BFA was reproduced when cells were pretreated with BDM for only 1–2 min or when BDM and BFA were added simultaneously. In both experimental conditions, BDM suppressed the effect of BFA (our unpublished data). Thus, the inhibition of the BFA-induced Golgi disassembly produced by BDM and ML7 is not merely the result of an alteration in calcium homeostasis.

Rho-Kinase Does Not Play a Role in Myosin II-based Golgi-to-ER Transport

Activation of myosin II via phosphorylation of the light chain can be regulated not only by MLCK but also by Rho kinase, which, in turn, is activated by RhoA-GTP directly phosphorylating MLC at Ser 19 or via inactivation of myosin phosphatase (Amano *et al.*, 1996; Kimura *et al.*, 1996; Kureishi *et al.*, 1997). To test whether Rho-dependent signaling, in addition to MLCK, plays a role in retrograde transport, we

assayed BFA-induced Golgi complex disassembly in cells that had been pretreated with Y-27632, a selective inhibitor of Rho-kinase (Uehata *et al.*, 1997), at concentrations of 25 and 50 μ M. Under these conditions, Y-27632 induced the disappearance of actin stress fibers (our unpublished data), but the Golgi complex morphology and the kinetics of the disassembly of the Golgi complex induced by BFA remained unaltered (Figure 3, M–Q). Thus, Rho-kinase does not play a role in myosin II activation during the Golgi-to-ER membrane flow and this activation is largely regulated by MLCK alone.

PIP5K-induced Actin Comets Mediate Neither in the Endocytic nor in the Golgi-to-ER Transport of ST-B

Activated Cdc42 regulates retrograde transport via N-WASP, which is recruited to the Golgi complex (Luna *et al.*, 2002). This suggests that an actin-based propulsion of transport carriers from Golgi to the ER is possible. To explore this possibility, we overexpressed myc-tagged PIP5K isotype I in cells by microinjection of its cDNA into the nucleus of HeLa cells, producing the appearance of filamen-

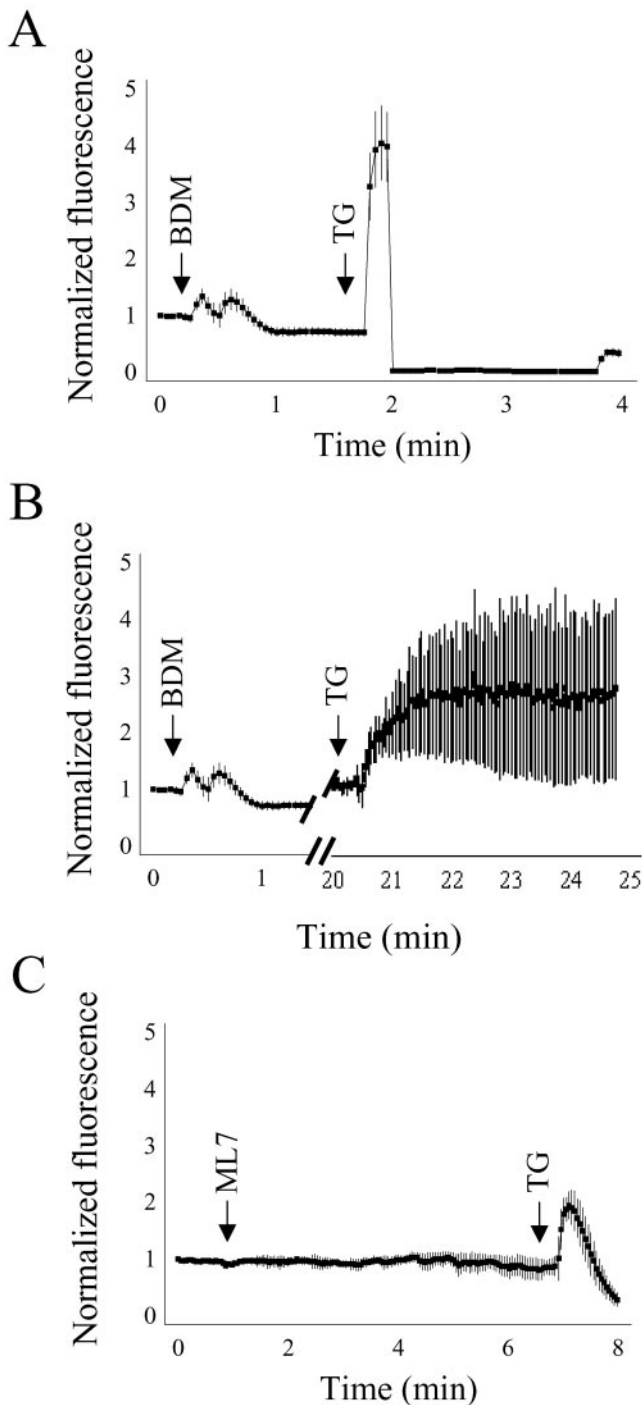


Figure 9. Representative traces showing the effect of BDM (20 mM) and ML7 (30 μ M) on intracellular calcium release in NRK cells. F4/AM-loaded cells were exposed to BDM (A and B) and ML7 (C). Notice that, unlike ML7, BDM induced a small and transient biphasic peak of $[Ca^{2+}]_i$ release. When thapsigargin (5 μ M) was subsequently added after 90 s (A) or 20 min (B), a second wave of $[Ca^{2+}]_i$ release was produced.

tous actin-containing comets as early as after 1 h of expression. To examine whether endocytic transport carriers were present at the heads of these actin comets, cells were first microinjected with PIP5K and, after 1–2 h of expression, they were incubated at 4°C with native Shiga toxin fragment B (ST-B). Subsequently, cells were washed and transferred to 37°C for short internalization times before chemical fixation (Figure 10). Confocal images showed that ST-B was not present at the heads of actin comets (Figure 10, A and A'). Next, we examined the membrane pathway from the Golgi complex to the ER. Cells were incubated with ST-B at 4°C for 30 min, washed, internalized at 37°C (at this temperature, ST-B shows a steady-state distribution at the Golgi complex, although it continuously and rapidly cycles through the ER), and finally PIP5K DNA was microinjected into the nucleus. Again, no transport carrier-containing ST-B colocalized with the head of actin comets (Figure 10, B and B'). PIP5K expression times longer than 3 h were unsatisfactory because the Golgi complex seemed extensively fragmented (our unpublished data). Taken together, these results strongly suggest that PIP5K-induced actin comets do not propel ST-B-containing transport carriers.

DISCUSSION

We have recently reported that actin facilitates Golgi-to-ER protein transport. Actin is present in the lateral rims of Golgi cisternae and in Golgi-derived transport intermediates (Valderrama *et al.*, 2000, 2001). In the present study, we have examined the mechanism supporting this physiological role of actin in trafficking between the ER and the Golgi. Currently, there are two possibilities; this involves either the actin-based motors or actin comets. We have tested which of these two processes is physiologically relevant in cultured mammalian cells, assuming that simultaneous action of both mechanisms in the Golgi-to-ER protein transport is unlikely. We used pharmacological and molecular experimental approaches to inhibit myosin motor activity or to generate actin comets. Our results can be summarized as follows: only the retrograde Golgi-to-ER pathway is inhibited when myosin motors are impaired; this alteration is not caused by changes in calcium homeostasis; and ST-B is not observed in the actin comet head at any time during its transport from the plasma membrane to the ER via the Golgi complex. Collectively, our results indicate that myosin motors and not actin comets are mediators of the actin-based Golgi-to-ER protein transport.

Actin-based Motors and Nonmuscle Myosin II in Golgi-to-ER Pathway

Myosins have been implicated in vesicular transport (for review, see Allan and Schroer, 1999). In particular, using BDM and a monoclonal antibody (AD7), it was reported that myosin II is involved in the formation of transport intermediates at the TGN (Müsch *et al.*, 1997). However, this result has been challenged by Simon *et al.* (1998), mainly because of the specificity of this antibody (see Stow *et al.*, 1998 for details). Additional experimental evidence that myosin II is the vesicle motor has been obtained by through use of ML7, a selective inhibitor of MLCK (Ruchhoeft and Harris, 1997). Inhibition of MLCK by ML7 blocks vesicle movement, pre-

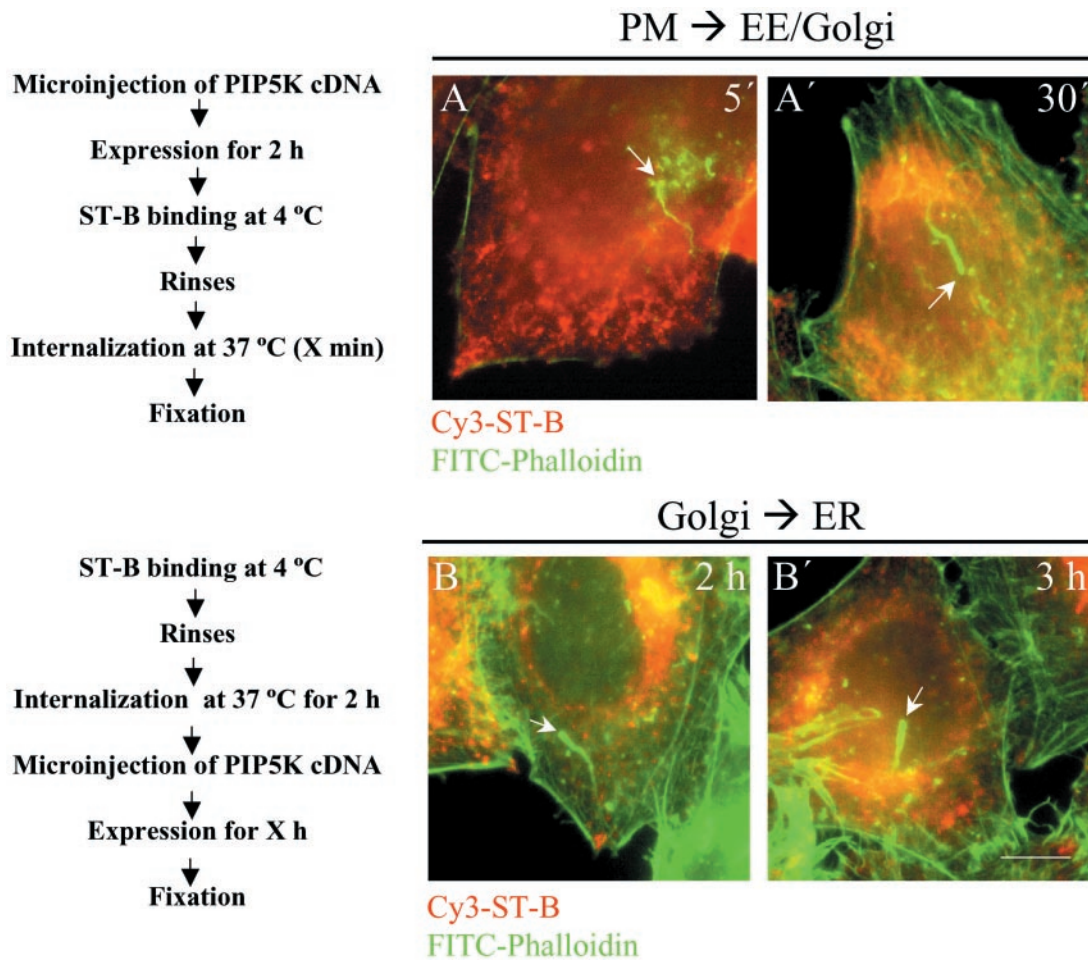


Figure 10. Merged images of PIP5K-overexpressed HeLa cells stained with fluorescein isothiocyanate-phalloidin (green) and cy3-ST-B (red). In A–A' and B–B', the transport route from the plasma membrane to early/recycling endosomes for ST-B and the Golgi-to-ER transport of ST-B were examined. Actin comets generated by overexpressing PIP5K were identified (white arrows). Notice that no association staining for two markers are observed in either of the experimental conditions, suggesting that actin comets do not propel ST-B at any stage of its internalization process to the ER. Bar, 10 μ m.

sumably by inhibiting the activity of myosin II (for review, see DePina and Langford, 1999). Hence, ML7 is a good reagent to test the involvement of myosin II in the biological processes examined. Herein, we observed that impairment in the BFA-induced disassembly of the Golgi complex is much more severe when cells are pretreated with BDM than with ML7. BDM could produce the higher inhibitory effect because of the simultaneous inhibition of several myosins (see below). The results with ML7 confirm those observed with BDM, but with the additional advantage that ML7 produced no alterations in the levels of intracellular calcium and was also more restrictive in the molecular target (myosin II). In this regard, the unaltered kinetics in the Golgi disassembly induced by BFA in cells treated with H89 and H7 suggest that neither PKA nor PKC are apparently involved in the Golgi-to-ER pathway. This is in accordance with the findings of Lee and Linstedt (2001), which despite the observation that the redistribution of Golgi residents to the ER was inhibited by H89 (at 50 μ M), they discarded that

PKA was the kinase required for the bidirectional transport at the ER/Golgi interface, because a number of other protein kinase inhibitors at concentrations reported to inhibit PKA and PKC (120 μ M H8; 9 μ M KT5720; 60 μ M H7) inhibited neither the retrograde nor anterograde transport. Thus, the use of ML7 at concentrations that are widely used in vivo are indicative that myosin II is involved in the retrograde protein transport. This was confirmed using a mutant of the nonmuscle myosin II regulatory light chain (MRLC2^{AA}) that cannot be phosphorylated. Cells transfected with this mutant showed similar perturbation in the Golgi disassembly induced by BFA treatment as that observed in ML7-treated cells (Figures 4 and 3, respectively). However, myosin II is neither a resident Golgi protein (Narula *et al.*, 1992; de Almeida *et al.*, 1993) nor a processive motor. These properties constrain its mode of action at the Golgi, and for this reason it has been suggested that the myosin II tail participates only in the budding of transport carriers (Stow *et al.*, 1998). Consequently, this assumption and the observation

that the delay in the Golgi disassembly induced by BFA is much more severe in BDM- than in ML7-treated cells, suggest the participation of a second (processive) motor that subsequently helps move the newly generated transport carriers to their final destination (in this case the ER). In this respect, myosins V and VI are processive motors (which means that it takes successive steps along the actin filament) that are reported to be located in the Golgi complex and involved in vesicular trafficking in some cell types (Nascimento *et al.*, 1997; Buss *et al.*, 1998; DePina and Langford, 1999; Miller and Sheetz, 2000; Schott *et al.*, 2002; da Silva Bizario *et al.*, 2002) and, thus, they could be acting in tandem with myosin II at the Golgi complex. However, we cannot completely rule out the sole implication of myosin II, because despite that this motor does not take successive steps along the actin filament, multiple myosin II moieties could show successive steps along a filament (a processive movement). This can occur if a second myosin II motor binds the filament before the first motor releases (Howard, 2001).

The observation that the emergence of tubules from the Golgi induced by BFA remains unaltered in BDM/ML7-treated cells suggests that actin motors are not directly involved in the formation of these tubules. Interestingly, BFA-induced tubules remain longer in the cytoplasm before their fusion with the ER. In addition, EM data suggest that myosin II is not directly involved in budding, because in ML7- and, to a lesser extent, BDM-treated cells, there is a significant accumulation of peri-Golgi vesicles (Table 1; Figure 2C), probably because they remain blocked in their movement to the ER once they have been formed at the lateral rims of the Golgi complex.

Taken together, these observations lead to the following three possibilities: 1) myosins are only involved in the locomotion process of transport carriers. Consequently, their inhibition delays the arrival of Golgi-derived transport carriers to putative ER entering sites; 2) transport carriers are normally transported via microtubules to the vicinity of these ER entering sites, but cannot be efficiently translocated to actin filaments, and their fusion to the ER is, therefore, delayed. Simultaneously, the BFA-induced tubules are continuously growing from the Golgi and become longer compared with those observed in control cells. This possibility suggests the presence of actin cytoskeleton and myosin motors associated with ER. The former has been reported in photoreceptor cells and in the corneal epithelium (Svoboda and Hay, 1987; Baumann and Lautenschlager, 1994); the latter is the case of myosin V, which is involved in the ER transport into the dendritic spines of neuronal cells (Tabb *et al.*, 1998; Molyneux *et al.*, 2000). However, we are not inclined for this possibility because first, we have not observed a significant association of β/γ -actin isoforms with ER membranes at the ultrastructural level by using monospecific polyclonal antibodies (J.A. Martínez-Menárguez and G. Egea, unpublished data); second, ST-B-KDEL is retained in the Golgi complex of cells with disrupted myosin function; and third, transport carriers are captured by peri-Golgi actin filaments via myosin motors as soon as they are formed at the lateral rims of Golgi cisternae. Subsequently, transport carriers are translocated to the microtubules for their movement to the ER. The presence of actin isoforms in Golgi-derived buds and vesicles (Valderrama *et al.*, 2000) and the accumulation of ST-B in the Golgi complex either when actin filaments are disrupted (Valderrama *et al.*, 2001) or myosin function is inhibited (this study) strongly support this possibility.

No Actin Comets in Golgi-to-ER Pathway

Plasma membrane and endomembranes are able to recruit N-WASP-Arp2/3 that could trigger focalized actin polymerization (actin tail), which in turn acts as a driving force for the locomotion of transport carriers or organelles (Merrifield *et al.*, 1999, 2001; Rozelle *et al.*, 2000; Taunton *et al.*, 2000; Lee and De Camilli, 2002; Benesch *et al.*, 2002; Orth *et al.*, 2002). Most of studies that report actin comets associated with endo/exocytic transport vesicles use cells that overexpress PIP5K (Rozelle *et al.*, 2000; Benesch *et al.*, 2002; Lee and De Camilli, 2002; Orth *et al.*, 2002). Using this same experimental approach, our results clearly show that transport carriers containing ST-B are not visualized at the head of actin tails during trafficking from plasma membrane to the ER (Figure 10). Nonetheless, small and short-lived actin comets could be generated concomitantly to the formation of transport carriers at the lateral rims of the Golgi, facilitating their final scission or separation from the cisternae. However, this possibility seems unlikely because the retrograde transport of ST-B and Golgi enzymes remained unaltered in cells expressing a truncated form of N-WASP lacking the Arp2/3 binding site and, therefore, unable to form actin comets (Luna *et al.*, 2002). These results, together with the previous observation that VSV-G is rarely associated with actin comets (Rozelle *et al.*, 2000), strongly indicate that actin comets do not propel transport carriers at the ER/Golgi interface.

In conclusion, our findings indicate that retrograde transport carriers use actin-based motors, most likely myosin II in their trafficking from Golgi membranes to the ER.

ACKNOWLEDGMENTS

We thank Laura Machesky for helpful discussions and PIP5-K1 α cDNA, and Montse Vilella for critically reading of the manuscript. We are also grateful to Bruno Goud, Hans-Peter Hauri, Eric Berger, and Kelley Moremen for antibodies and reagents; Robin Rycroft for editorial assistance; Maite Muñoz for skillful technical assistance; and Serveis Científic-Tècnics de la Universitat de Barcelona (Campus Casanova) for help with confocal microscope. The work in the laboratory of G.E. is supported by grants from Comisión Interministerial de Ciencia y Tecnológica (SAF2000-0042) and Comissió Interdepartamental de Recerca i Innovació Tecnològica (AGP2002). J.D., F.V., and M.T. are recipients of predoctoral fellowships from Fondo de Investigaciones Sanitarias, Universitat de Barcelona, and Ministerio de Educación y Ciencia, respectively. G.E. dedicates this article to the memory of the innocent victims of terrorist attacks wherever they occur.

REFERENCES

- Allan, V.J., and Schroer, T.A. (1999). Membrane motors. *Curr. Opin. Cell Biol.* 11, 476–482.
- Amano, M., Ito, M., Kimura, K., Fukata, Y., Chihara, K., Nakano, T., Matsuura, Y., and Kaibuchi, K. (1996). Phosphorylation and activation of myosin by Rho-associated kinase (Rho-kinase). *J. Biol. Chem.* 271, 20246–20249.
- Apodaca, G. (2001). Endocytic traffic in polarized epithelial cells: role of the actin and microtubule cytoskeleton. *Traffic* 2, 149–159.
- Baumann, O., and Lautenschlager, B. (1994). The role of actin filaments in the organization of the endoplasmic reticulum in honeybee photoreceptor cells. *Cell Tissue Res.* 278, 419–432.

- Beckers, C.J., and Balch, W.E. (1989). Calcium and GTP: essential components in vesicular trafficking between the endoplasmic reticulum and Golgi apparatus. *J. Cell Biol.* *108*, 1245–1256.
- Benesch, S., Lommel, S., Steffen, A., Stradal, T.E., Scaplehorn, N., Way, M., Wehland, J., and Rottner, K. (2002). PIP2-induced vesicle movement depends on N-WASP and involves Nck, WIP and Grb2. *J. Biol. Chem.* *277*, 37771–37776.
- Bonatti, S., Migliaccio, G., and Simons, K. (1989). Palmitoylation of viral membrane glycoproteins takes place after exit from the endoplasmic reticulum. *J. Biol. Chem.* *264*, 12590–12595.
- Bootman, M., Niggli, E., Berridge, M., and Lipp, P. (1997). Imaging the hierarchical Ca^{2+} signaling system in HeLa cells. *J. Physiol.* *499*, 307–314.
- Buss, F., Kendrick-Jones, J., Lionne, C., Knight, A.E., Cote, G.P., and Paul, L.J. (1998). The localization of myosin VI at the Golgi complex and leading edge of fibroblasts and its phosphorylation and recruitment into membrane ruffles of A431 cells after growth factor stimulation. *J. Cell Biol.* *143*, 1535–1545.
- Buss, F., Arden, S.D., Lindsay, M., Luzio, J.P., and Kendrick-Jones, J. (2001). Myosin VI isoform localized to clathrin-coated vesicles with a role in clathrin-mediated endocytosis. *EMBO J.* *20*, 3676–3684.
- Chen, J.L., Ahluwalia, J.P., and Stamnes, M. (2002). Selective effects of calcium chelators on anterograde- and retrograde-protein transport in the cell. *J. Biol. Chem.* *277*, 35682–35687.
- Cordonnier, M.N., Dauzonne, D., Louvard, D., and Coudrier, E. (2001). Actin filaments and myosin I alpha cooperate with microtubules for the movement of lysosomes. *Mol. Biol. Cell* *12*, 4013–4029.
- Cossart, P. (2000). Actin-based motility of pathogens: the Arp2/3 complex is a central player. *Cell Microbiol.* *2*, 195–205.
- Cramer, L.P., and Mitchison, T.J. (1995). Myosin is involved in postmitotic cell spreading. *J. Cell Biol.* *131*, 179–189.
- da Silva Bizario, J.C., da Cunha Nascimento, A.A., Casaletti, L., Patussi, E.V., Chociay, M.F., Larson, R.E., and Espreafico, E.M. (2002). Expression of constructs of the neuronal isoform of myosin-Va interferes with the distribution of melanosomes and other vesicles in melanoma cells. *Cell Motil. Cytoskeleton* *51*, 57–75.
- de Almeida, J.B., Doherty, J., Ausiello, D.A., and Stow, J.L. (1993). Binding of the cytosolic p200 protein to Golgi membranes is regulated by heterotrimeric G proteins. *J. Cell Sci.* *106*, 1239–1248.
- De Matteis, M.A., and Morrow, J.S. (2000). Spectrin tethers and mesh in the biosynthetic pathway. *J. Cell Sci.* *113*, 2331–2343.
- DePina, A.S., and Langford, G.M. (1999). Vesicle transport: the role of actin filaments and myosin motors. *Microsc. Res. Tech.* *47*, 93–106.
- Donaldson, J.G., Lippincott-Schwartz, J., Bloom, G.S., Kreis, T.E., and Klausner, R.D. (1990). Dissociation of a 110-kD peripheral membrane protein from the Golgi apparatus is an early event in brefeldin A action. *J. Cell Biol.* *111*, 2295–2306.
- Ecay, T.W., Conner, T.D., and Decker, E.R. (1997). Nonmuscle myosin IIA copurifies with chloride channel-enriched membranes from epithelia. *Biochem. Biophys. Res. Commun.* *231*, 369–372.
- Fath, K., and Burgess, D. (1993). Golgi-derived vesicles from developing epithelial cells bind actin filaments and possess myosin-I as a cytoplasmically oriented peripheral membrane protein. *J. Cell Biol.* *120*, 117–127.
- Fath, K.R., Trimbur, G.M., and Burgess, D.R. (1994). Molecular motors are differentially distributed on Golgi membranes from polarized epithelial cells. *J. Cell Biol.* *126*, 661–675.
- Gloushankova, N.A., Krendel, M.F., Alieva, N.O., Bonder, E.M., Feder, H.H., Vasiliev, J.M., and Gelfand, I.M. (1998). Dynamics of contacts between lamellae of fibroblasts: essential role of the actin cytoskeleton. *Proc. Natl. Acad. Sci. USA* *95*, 4362–4367.
- Goldberg, M.B. (2001). Actin-based motility of intracellular microbial pathogens. *Microbiol. Mol. Biol. Rev.* *65*, 595–626.
- Heemskerck, J.W., Willems, G.M., Rook, M.B., and Sage, S.O. (2001). Ragged spiking of free calcium in ADP-stimulated human platelets: regulation of puff-like calcium signals in vitro and ex vivo. *J. Physiol.* *535*, 625–635.
- Heimann, K., Percival, J.M., Weinberger, R., Gunning, P., and Stow, J.L. (1999). Specific isoforms of actin-binding proteins on distinct populations of Golgi-derived vesicles. *J. Biol. Chem.* *274*, 10743–10750.
- Herrmann, C., Wray, J., Travers, F., and Barman, T. (1992). Effect of 2,3-butanedione monoxime on myosin and myofibrillar ATPases. An example of an uncompetitive inhibitor. *Biochemistry* *31*, 12227–12232.
- Higuchi, H., and Takemori, S. (1989). Butanedione monoxime suppresses contraction and ATPase activity of rabbit skeletal muscle. *J. Biochem.* *105*, 638–643.
- Howard, J. (2001). *Mechanics of Motor Proteins and the Cytoskeleton*, London, England: Palgrave Macmillian.
- Ikonen, E., Parton, R.G., Lafont, F., and Simons, K. (1996). Analysis of the role of p200-containing vesicles in post-Golgi traffic. *Mol. Biol. Cell* *7*, 961–974.
- Ikonen, E., de Almeida, J.B., Fath, K.R., Burgess, D.R., Ashman, K., Simons, K., and Stow, J.L. (1997). Myosin II is associated with Golgi membranes: identification of p200 as nonmuscle myosin II on Golgi-derived vesicles. *J. Cell Sci.* *110*, 2155–2164.
- Ivessa, N.E., De Lemos-Chiarandini, C., Gravota, D., Sabatini, D.D., and Kreibich, G. (1995). The brefeldin A-induced retrograde transport from the Golgi apparatus to the endoplasmic reticulum depends on calcium sequestered to intracellular stores. *J. Biol. Chem.* *270*, 25960–25967.
- Iwasaki, T., Murata-Hori, M., Ishitobi, S., and Hosoya, H. (2001). Diphosphorylated MRLC is required for organization of stress fibers in interphase cells, and the contractile ring in dividing cells. *Cell Struct. Funct.* *26*, 677–683.
- Johannes, L., Tenza, D., Anthony, C., and Goud, B. (1997). Retrograde transport of KDEL-bearing B-fragment of Shiga toxin. *J. Biol. Chem.* *272*, 19554–19561.
- Kimura, K., *et al.* (1996). Regulation of myosin phosphatase by Rho and Rho-associated kinase (Rho-kinase). *Science* *273*, 245–248.
- Kureishi, Y., Kobayashi, S., Amano, M., Kimura, K., Kanaide, H., Nakano, T., Kaibuchi, K., and Ito, M. (1997). Rho-associated kinase directly induces smooth muscle contraction through myosin light chain phosphorylation. *J. Biol. Chem.* *272*, 12257–12260.
- Lamb, N.J., Fernandez, A., Conti, M.A., Adelstein, R., Glass, D.B., Welch, W.J., and Feramisco, J.R. (1988). Regulation of actin microfilament integrity in living nonmuscle cells by the cAMP-dependent protein kinase and the myosin light chain kinase. *J. Cell Biol.* *106*, 1955–1971.
- Lee, E., and De Camilli, P. (2002). Dynamin at actin tails. *Proc. Natl. Acad. Sci. USA* *99*, 161–166.
- Lee, T.H., and Linstedt, A.D. (2000). Potential role for protein kinases in regulation of bidirectional endoplasmic reticulum-to-Golgi transport revealed by protein kinase inhibitor H89. *Mol. Biol. Cell* *11*, 2577–2790.
- Lin, C.H., Espreafico, E.M., Mooseker, M.S., and Forscher, P. (1996). Myosin drives retrograde F-actin flow in neuronal growth cones. *Neuron* *16*, 769–82.
- Luna, A., Matas, O.B., Martínez-Menárguez, J.A., Mato, E., Durán, J.M., Ballesta, J., Way, M., and Egea, G. (2002). Regulation of protein transport from the Golgi complex to the endoplasmic reticulum by cdc42 and N-WASP. *Mol. Biol. Cell* *13*, 866–879.

- May, R.C., and Machesky, L.M. (2001). Phagocytosis and the actin cytoskeleton. *J. Cell Sci.* 114, 1061–1077.
- Merrifield, C.J., Moss, S.E., Ballestrem, C., Imhof, B.A., Giese, G., Wunderlich, I., and Almers, W. (1999). Endocytic vesicles move at the tips of actin tails in cultured mast cells. *Nat. Cell Biol.* 1, 72–74.
- Merrifield, C.J., Rescher, U., Almers, W., Proust, J., Gerke, V., Sechi, A.S., and Moss, S.E. (2001). Annexin 2 has an essential role in actin-based macropinocytic rocketing. *Curr. Biol.* 11, 1136–1141.
- Miller, K.E., and Sheetz, M.P. (2000). Characterization of myosin V binding to brain vesicles. *J. Biol. Chem.* 275, 2598–2606.
- Molyneaux, B.J., Mulcahey, M.K., Stafford, P., and Langford, G.M. (2000). Sequence and phylogenetic analysis of squid myosin-V: a vesicle motor in nerve cells. *Cell Motil. Cytoskeleton* 46, 108–115.
- Montes de Oca, G., Lezama, R.A., Mondragón, R., Castillo, A.M., and Meza, I. (1997). Myosin I interactions with actin filaments, and trans-Golgi-derived vesicles in MDCK cell monolayers. *Arch. Med. Res.* 28, 321–328.
- Müsch, A., Cohen, D., and Rodriguez-Boulan, E. (1997). Myosin II is involved in the production of constitutive transport vesicles from the TGN. *J. Cell Biol.* 138, 291–306.
- Müsch, A., Cohen, D., Kreitzer, G., and Rodriguez-Boulan, E. (2001). Cdc42 regulates the exit of apical and basolateral proteins from the trans-Golgi network. *EMBO J.* 20, 2171–2179.
- Narula, N., and Stow, J.L. (1995). Distinct coated vesicles labeled for p200 bud from trans-Golgi network membranes. *Proc. Natl. Acad. Sci. USA* 92, 2874–2878.
- Narula, N., McMorrow, I., Plopper, G., Doherty, J., Matlin, K.S., Burke, B., and Stow, J.L. (1992). Identification of a 200-kD, brefeldin-sensitive protein on Golgi membranes. *J. Cell Biol.* 117, 27–38.
- Nascimento, A.A., Amaral, R.G., Bizario, J.C., Larson, R.E., and Esprefaco, E.M. (1997). Subcellular localization of myosin-V in the B16 melanoma cells, a wild-type cell line for the dilute gene. *Mol. Biol. Cell* 8, 1971–1988.
- Orth, J.D., Krueger, E.W., Cao, H., and McNiven, M.A. (2002). The large GTPase dynamin regulates actin comet formation and movement in living cells. *Proc. Natl. Acad. Sci. USA* 99, 67–72.
- Phillips, R.M., and Altschuld, R.A. (1996). 2,3-Butanedione 2-monoxime (BDM) induces calcium release from canine cardiac sarcoplasmic reticulum. *Biochem. Biophys. Res. Commun.* 229, 154–157.
- Prekeris, R., and Terrian, D.M. (1997). Brain myosin V is a synaptic vesicle-associated motor protein: evidence for a Ca²⁺-dependent interaction with the synaptobrevin-synaptophysin complex. *J. Cell Biol.* 137, 1589–1601.
- Qualmann, B., Kessels, M.M., and Kelly, R.B. (2000). Molecular links between endocytosis and the actin cytoskeleton. *J. Cell Biol.* 150, F111–F116.
- Ridley, A.J. (2001). Rho proteins: linking signaling with membrane trafficking. *Traffic* 2, 303–310.
- Renau-Piqueras, J., Miragall, F., Guerri, C., and Baguena-Cervellera, R. (1987). Prenatal exposure to alcohol alters the Golgi apparatus of newborn rat hepatocytes: a cytochemical study. *J. Histochem. Cytochem.* 35, 221–228.
- Rozelle, A.L., Machesky, L.M., Yamamoto, M., Driessens, M.H., Insall, R.H., Roth, M.G., Luby-Phelps, K., Marriott, G., Hall, A., and Yin, H.L. (2000). Phosphatidylinositol 4,5-bisphosphate induces actin-based movement of raft-enriched vesicles through WASP-Arp2/3. *Curr. Biol.* 10, 311–320.
- Ruchhoeft, M.L., and Harris, W.A. (1997). Myosin functions in *Xenopus* retinal ganglion cell growth cone motility in vivo. *J. Neurobiol.* 32, 567–578.
- Saitoh, M., Ishikawa, T., Matsushima, S., Naka, M., and Hidaka, H. (1987). Selective inhibition of catalytic activity of smooth muscle myosin light chain kinase. *J. Biol. Chem.* 262, 7796–7801.
- Sandvig, K., and van Deurs, B. (2000). Entry of ricin and Shiga toxin into cells: molecular mechanisms and medical perspectives. *EMBO J.* 19, 5943–5950.
- Svoboda, K.K., and Hay, E.D. (1987). Embryonic corneal epithelial interaction with exogenous laminin and basal lamina is F-actin dependent. *Dev. Biol.* 123, 455–469.
- Scheel, J., Pepperkok, R., Lowe, M., Griffiths, G., and Kreis, T.E. (1997). Dissociation of coatamer from membranes is required for brefeldin A-induced transfer of Golgi enzymes to the endoplasmic reticulum. *J. Cell Biol.* 137, 319–333.
- Schott, D.H., Collins, R.N., and Bretscher, A. (2002). Secretory vesicle transport velocity in living cells depends on the myosin-V lever arm length. *J. Cell Biol.* 156, 35–39.
- Sciaky, N., Presley, J., Smith, C., Zaal, K.J., Cole, N., Moreira, J.E., Terasaki, M., Siggia, E., and Lippincott-Schwartz, J. (1997). Golgi tubule traffic and the effects of brefeldin A visualized in living cells. *J. Cell Biol.* 139, 1137–1155.
- Simon, J.P., Shen, T.H., Ivanov, I.E., Gravotta, D., Morimoto, T., Adesnik, M., and Sabatini, D.D. (1998). Coatamer, but not P200/myosin II, is required for the in vitro formation of trans-Golgi network-derived vesicles containing the envelope glycoprotein of vesicular stomatitis virus. *Proc. Natl. Acad. Sci. USA* 95, 1073–1078.
- Stamnes, M. (2002). Regulating the actin cytoskeleton during vesicular transport. *Curr. Opin. Cell Biol.* 14, 428–433.
- Steinberg, G., and McIntosh, J.R. (1998). Effects of the myosin inhibitor 2,3-butanedione monoxime on the physiology of fission yeast. *Eur. J. Cell Biol.* 77, 284–293.
- Stow, J.L., Fath, K.R., and Burgess, D.R. (1998). Budding roles for myosin II on the Golgi. *Trends Cell Biol.* 8, 138–141.
- Tabb, J.S., Molyneaux, B.J., Cohen, D.L., Kuznetsov, S.A., and Langford, G.M. (1998). Transport of ER vesicles on actin filaments in neurons by myosin V. *J. Cell Sci.* 111, 3221–3234.
- Taunton, J., Rowning, B.A., Coughlin, M.L., Wu, M., Moon, R.T., Mitchison, T.J., and Larabell, C.A. (2000). Actin-dependent propulsion of endosomes and lysosomes by recruitment of N-WASP. *J. Cell Biol.* 148, 519–530.
- Taunton, J. (2001). Actin filament nucleation by endosomes, lysosomes and secretory vesicles. *Curr. Opin. Cell Biol.* 13, 85–91.
- Thastrup, O., Cullen, P.J., Drobak, B.K., Hanley, M.R., and Dawson, A.P. (1990). Thapsigargin, a tumor promoter, discharges intracellular Ca²⁺ stores by specific inhibition of the endoplasmic reticulum Ca²⁺(+)-ATPase. *Proc. Natl. Acad. Sci. USA* 87, 2466–2470.
- Uehata, M., Ishizaki, T., Satoh, H., Ono, T., Kawahara, T., Morishita, T., Tamakawa, H., Yamagami, K., Inui, J., Maekawa, M., and Narumiya, S. (1997). Calcium sensitization of smooth muscle mediated by a Rho-associated protein kinase in hypertension. *Nature* 389, 990–994.
- Valderrama, F., Babià, T., Ayala, I., Kok, J.W., Renau-Piqueras, J., and Egea, G. (1998). Actin microfilaments are essential for the cytological positioning and morphology of the Golgi complex. *Eur. J. Cell Biol.* 76, 9–17.
- Valderrama, F., Luna, A., Babià, T., Martínez-Menárguez, J.A., Ballasta, J., Barth, H., Chaponnier, C., Renau-Piqueras, J., and Egea, G. (2000). The Golgi-associated COPI-coated buds and vesicles contain β/γ -actin. *Proc. Natl. Acad. Sci. USA* 97, 1560–1565.
- Valderrama, F., Durán, M., Babià, T., Barth, H., Renau-Piqueras, J., and Egea, G. (2001). Actin microfilaments facilitate the retrograde transport from the Golgi complex to the endoplasmic reticulum in mammalian cells. *Traffic* 2, 717–726.